REPORT DOCUMENTATION PAGE

Form Approved
OMB No. 0704-0188

1. REPORT DATE *(DD-MM-YYYY)*
Oct 2006

2. REPORT TYPE
Journal Article Postprint

3. DATES COVERED *(From - To)*
2006

4. TITLE AND SUBTITLE
First Demonstration of ~10 microns FPAs in InAs/GaSb SLS

5a. CONTRACT NUMBER

5b. GRANT NUMBER

5c. PROGRAM ELEMENT NUMBER

Manijeh Razeghi,* Pierre-Yves Delaunay, Binh Minh Nguyen, Andrew Hood, Darin Hoffman, Ryan McClintock, Yajun Wei, Erick Michel, Vaidya Nathan,** Meimei Z. Tidrow***

5d. PROJECT NUMBER

5e. TASK NUMBER

5f. WORK UNIT NUMBER

7. PERFORMING ORGANIZATION NAME(S) AND ADDRESS(ES)

Center for Quantum Devices*
EECS Department
Northwestern University
Evanston, IL 60208

Missile Defense Agency***
7100 Defense Pentagon
Washington, DC 20301

8. PERFORMING ORGANIZATION REPORT NUMBER

9. SPONSORING / MONITORING AGENCY NAME(S) AND ADDRESS(ES)

Air Force Research Laboratory**
Space Vehicles Dirctorate
3550 Aberdeen Ave SE
Kirtland AFB, NM 87117-5776

10. SPONSOR/MONITOR'S ACRONYM(S)
AFRL/VSSS

11. SPONSOR/MONITOR'S REPORT NUMBER(S)
AFRL-VS-PS-JA-2007-1002

12. DISTRIBUTION / AVAILABILITY STATEMENT
Approved for public release; distribution is unlimited. (Clearance #VS06-0748)

13. SUPPLEMENTARY NOTES
Published in the IEEE LEOS Newsletter, Oct 2006, Vol 20, No 5, pp 43-46.

Government Purpose Rights

14. ABSTRACT
The concept of Type II InAs/GaSb superlattice was first brought by Nobel Laureate L. Esaki, et al. in the 1970s. There had been few studies on this material system until two decades later when reasonable quality material growth was made possible using molecular beam epitaxy. With the addition of cracker cells for the group V sources and optimizations of material growth conditions, the super lattice quality become significantly improved and the detectors made of these super lattice material can meet the demand in some practical field applications. Especially in the LWIR regime, it provides a very promising alternative to HgCdTe for better material stability and uniformity etc. We have developed the empirical tight binding model (ETBM) for precise determination of the superlattice bandgap. New concept of A1Sb contained M-structure superlattice has been added to enhance the wavelength tunability. We have recently demonstrated diodes with 50% cutoff wavelength of 12 µm at liquid nitrogen temperature. The R_0A of these diodes reached as high as 33 ohm·cm^2 and device quantum efficiency of 40-50% with D* around 2×10^{11} cm·Hz$^{1/2}$/W. We have also demonstrated the first FPA with 50% cutoff wavelength around 10 µm.

15. SUBJECT TERMS
FPA, InAs/GaSb superlattices, infrared material, focal plane arrays, mesa, 10 micron, InAs-GaSb

16. SECURITY CLASSIFICATION OF:			17. LIMITATION OF ABSTRACT	18. NUMBER OF PAGES	19a. NAME OF RESPONSIBLE PERSON
a. REPORT	**b. ABSTRACT**	**c. THIS PAGE**			Vaidya Nathan
Unclassified	Unclassified	Unclassified	Unlimited	5	**19b. TELEPHONE NUMBER** *(include area code)* 505-846-4497

Standard Form 298 (Rev. 8-98)
Prescribed by ANSI Std. 239.18

First Demonstration of ~10 microns FPAsin InAs/GaSb SLS

Manijeh Razeghi, Pierre-Yves Delaunay, Binh Minh Nguyen, Andrew Hood, Darin Hoffman, Ryan McClintock, Yajun Wei, Erick Michel, Vaidya Nathan**, Meimei Z. Tidrow****

Abstract

The concept of Type II InAs/GaSb superlattice was first brought by Nobel Laureate L. Esaki, et al. in the 1970s. There had been few studies on this material system until two decades later when reasonable quality material growth was made possible using molecular beam epitaxy. With the addition of cracker cells for the group V sources and optimizations of material growth conditions, the superlattice quality become significantly improved and the detectors made of these superlattice material can meet the demand in some practical field applications. Especially in the LWIR regime, it provides a very promising alternative to HgCdTe for better material stability and uniformity etc. We have developed the empirical tight binding model (ETBM) for precise determination of the superlattice bandgap. New concept of AlSb contained M-structure superlattice has been added to enhance the wavelength tunability. We have recently demonstrated diodes with 50% cutoff wavelength of 12 μm at liquid nitrogen temperature. The R_0A of these diodes reached as high as 33 $\Omega \cdot cm^2$ and device quantum efficiency of 40-50%. with D* around 2×10^{11} $cm \cdot Hz^{1/2}/W$. We have also demonstrated the first FPA with 50% cutoff wavelength around 10 μm.

Introduction

Type II InAs/GaSb superlattices, first introduced in 1971 by Sai-Halasz and L. Esaki et al.,[1] feature a misaligned bandgap, where the conduction band of InAs is below the valence band of GaSb. As a result, on the contrary of Type I superlattices, carriers are not confined in the same layers. Because of this misalignment, the effective bandgap of the material is smaller than the bandgap of each of its constituents. By changing the number of layers of InAs and GaSb in each period, it is theoretically possible to tune the gap between 0 and 0.3 eV[2] We have demonstrated superlattices with cutoff wavelength between 3.7 μm and 32 μm[3,4]. The atmospheric transmission window between 8 – 12 μm is of particular interest since room temperature objects emit most infrared radiation around 10 μm. This leads to numerous applications for LWIR imaging such as long range target detection, non-destructive examinations in medical fields and industry. In this wavelength regime, the Type II superlattice is a very promising alternative to HgCdTe. The superlattice material can have better material uniformity and stability due to the stronger chemical bonding between group III and V elements. Tunable bandstructure and separation of electrons and holes will make reduction of Auger recombination possible in the superlattice material. This will make higher operating temperature possible.

Empirical Tight Binding Model

To direct our design efficiently, we have been using an Empirical Tight Binding Model (ETBM)[5,6] that allows us to reach the desired cutoff wavelength. This model includes effects of strain, different types of interfaces. The effectiveness and accuracy of this model has been confirmed experimentally by numerous growths. A new Type II structure, called "M" structure as illustrated in Figure 1, is currently under investigation for higher performance infrared photodetectors. This structure, constructed by inserting an AlSb barrier in the middle of the GaSb layer in a normal type II superlattice, suggests many promising properties relevant to practical use. Firstly, the AlSb barriers decrease the electron mobility by blocking the diffusion mechanism in the conduction band. This decrease of the mobility reduces the dark current and improves the R_0A product of the photodiodes. Secondly, the AlSb layer is also a

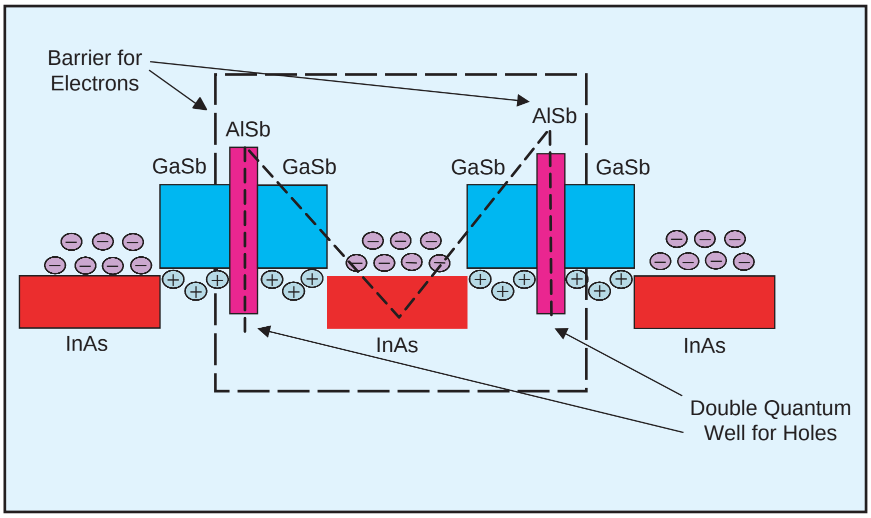

Figure 1 Band alignment diagram for a Type II "M" structure. Varying the position of AlSb will change the superlattice bandgap without material composition change.

CENTER FOR QUANTUM DEVICES, EECS DEPARTMENT, NORTHWESTERN UNIVERSITY, EVANSTON, IL 60208, USA
* ELECTRONIC MAIL: RAZEGHI@ECE.NORTHWESTERN.EDU
** AIR FORCE RESEARCH LABORATORY/VSSS, KIRTLAND AIR FORCE BASE, NEW MEXICO 87117
*** MISSILE DEFENSE AGENCY, 7100 DEFENSE PENTAGON, WASHINGTON, DC 20301

barrier for holes in the conduction band, pushing them toward the interface between the InAs and the GaSb layers. The wavefunction overlap of electron and holes is increased, thus, the internal quantum efficiency is improved. Thirdly, we have successfully demonstrated a new bandgap engineering method by shifting the position of the AlSb barrier in the GaSb layer. This method allows shifting the cut-off wavelength of the structure about 2 µm without changing the lattice mismatch and the composition of the material. Finally, in the point of view of material growth, this structure has the simplicity of a binary structure. A typical ETBM bandstructure is shown in Figure 2.

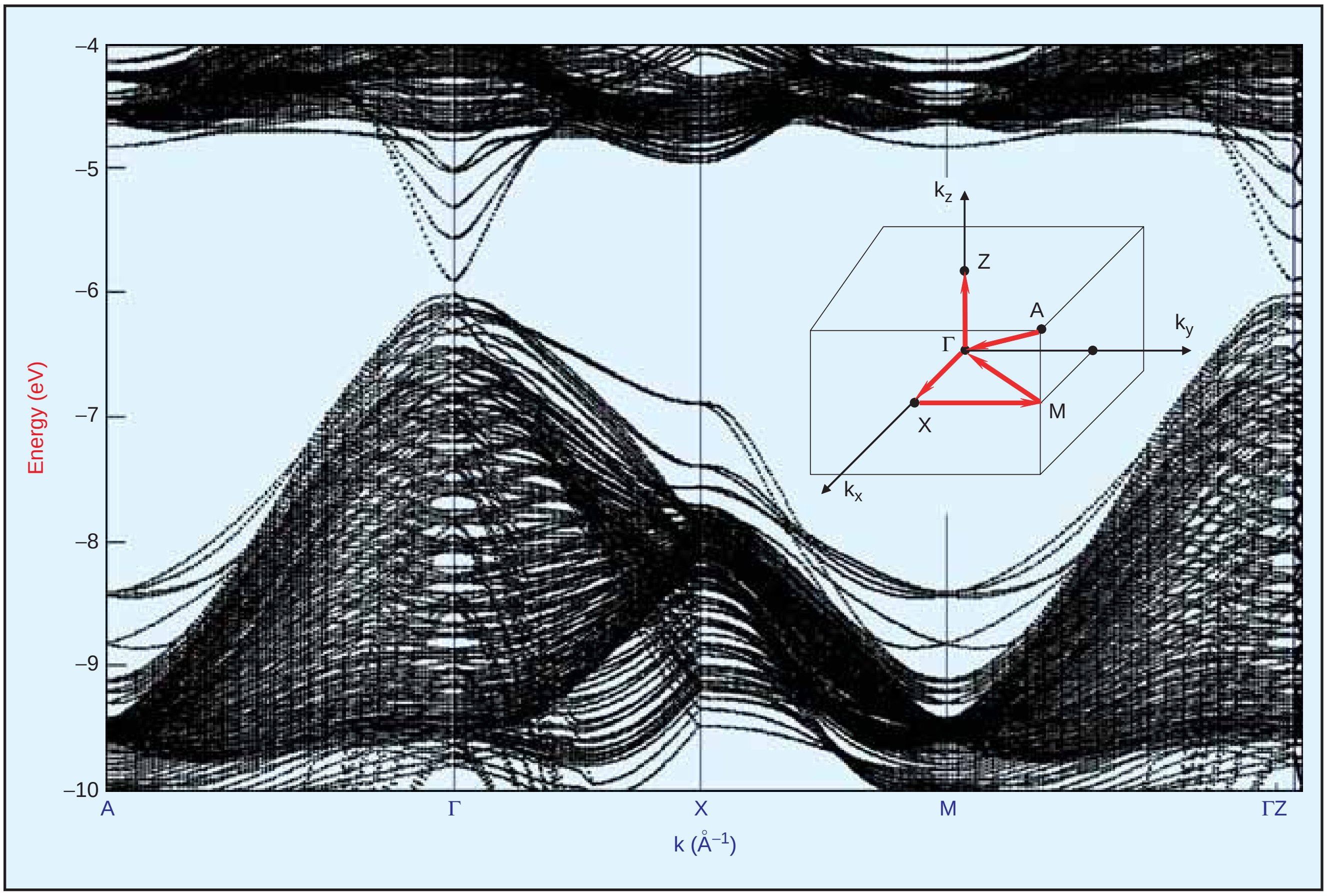

Figure 2 Typical bandstructure of a Type II "M" structure superlattice.

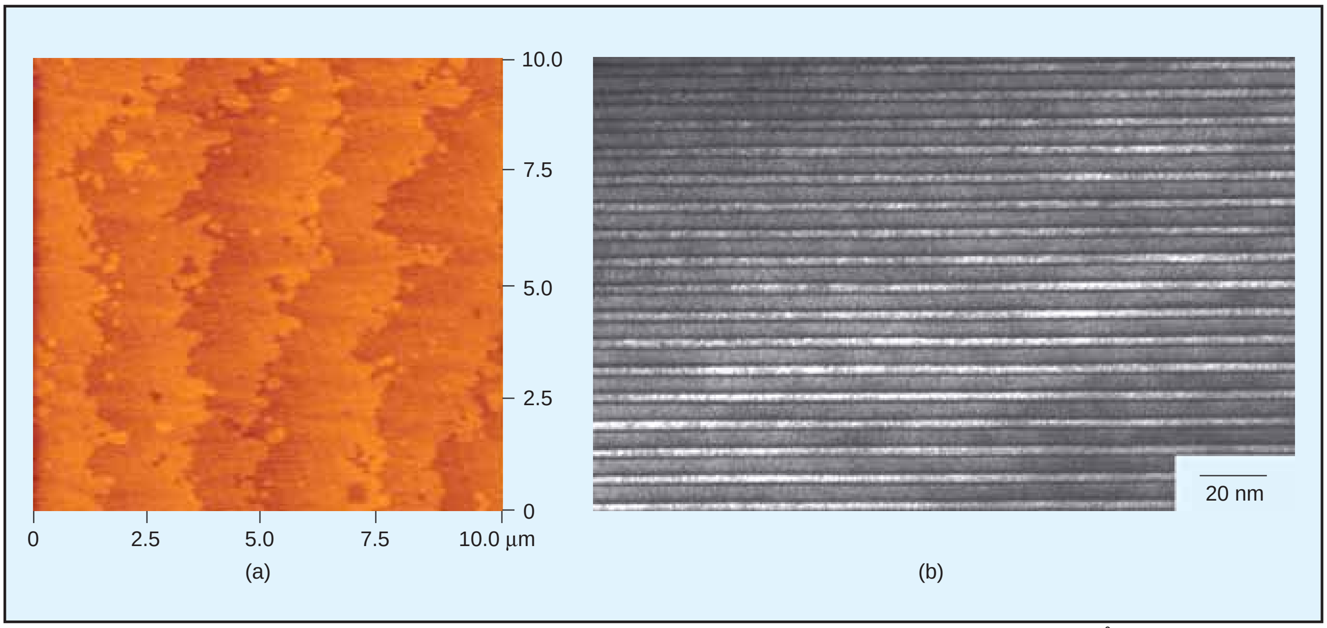

Figure 3 Material characterization using (a) AFM and (b) TEM. Surface RMS roughness reached around 1.1-1.6Å.

Material growth and characterization

Type II superlattices are grown using a Intevac Gen II Molecular Beam Epitaxy system (now part of Veeco) equipped with valved cracker source for group V elements and SUMO cells for In and Ga. Firstly, a 0.5 µm GaSb buffer is deposited on a p-type epi-ready GaSb (001) substrate to smooth out the surface. Next, a 0.5 µm etch stop layer: InAsSb latticed matched with GaSb is grown for substrate removal purpose. A

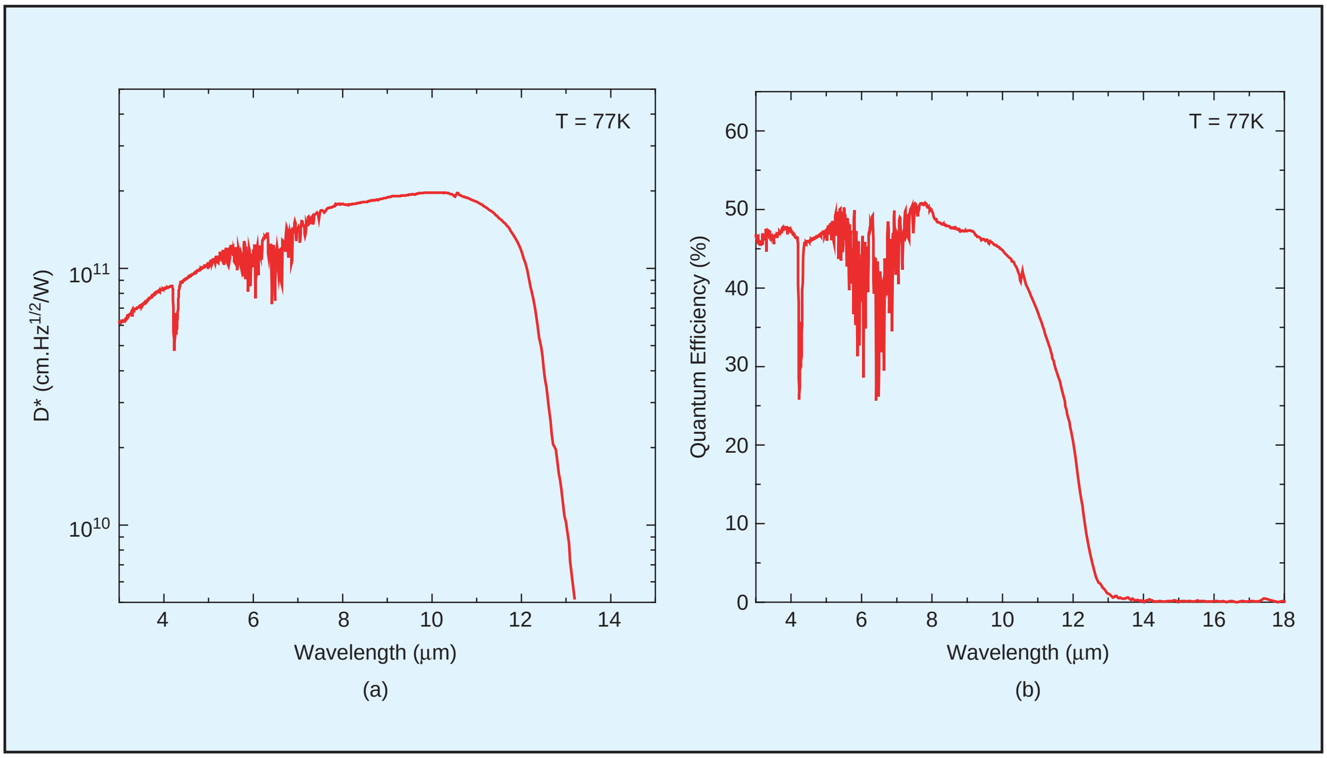

Figure 4 Device performance of the 12 µm cutoff photodiodes. Average D reached ~2×10^{11} cm·Hz$^{1/2}$/W (a), and average device quantum efficiency reached 40-50% (b). CO_2 and H_2O bands are shown in the spectrum.*

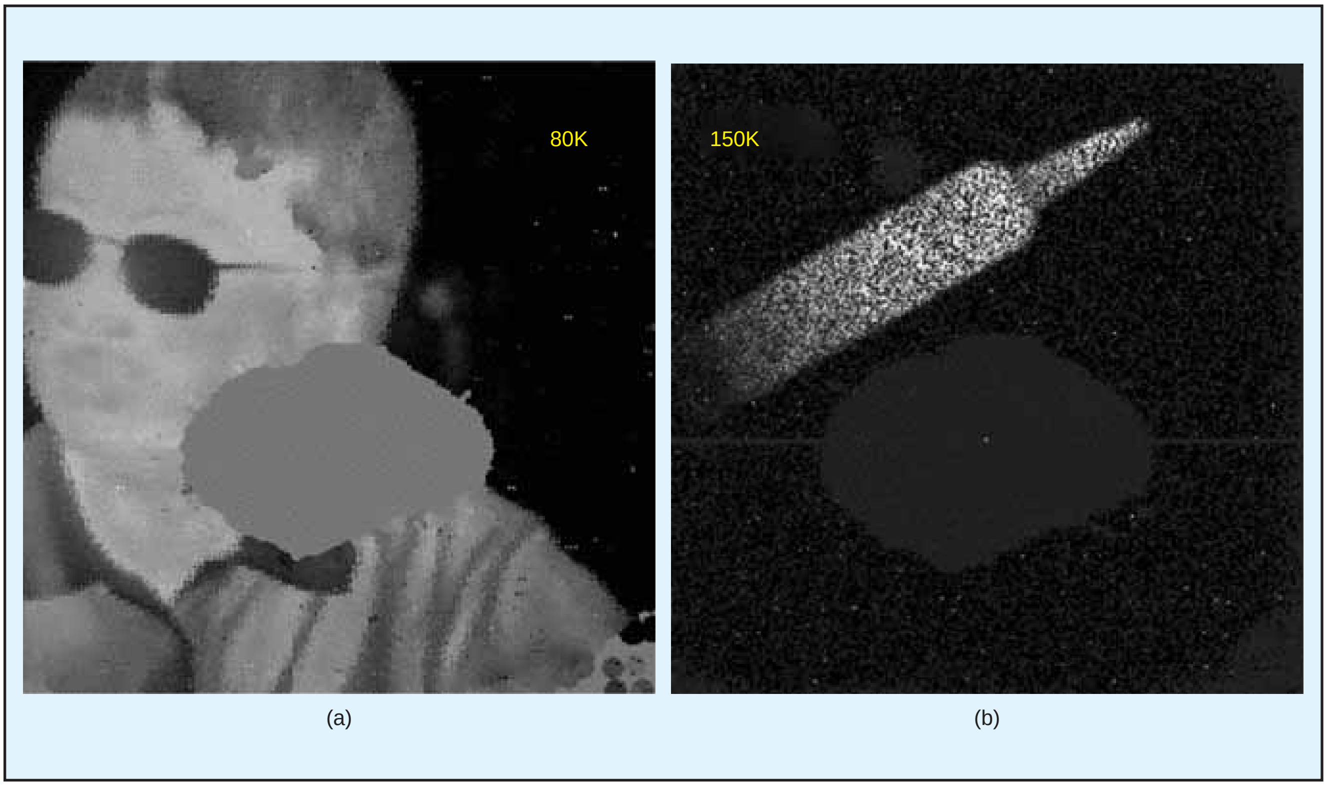

Figure 5 Infrared imaging obtained at (a) 80K and (b) 150K.

p-i-n superlattice structure with respective layer thickness of 0.5 µm, 2 µm and 0.5 µm, was then deposited and capped by 10 nm of InAs n+ for top contact. The p and n regions are doped at 10^{18} cm^{-3} while the i region is nominally undoped. The growth temperature is around 500°C, according to a calibrated pyrometer, for the GaSb buffer and the InAsSb etch stop layer, and 400°C for the superlattice.

Structural characterization is performed to prove the high quality of grown materials. AFM images show wide atomic steps. An example is shown in Figure 3(a). A roughness of 1.1-1.6 Å can be routinely achieved for a scan size of 20 µm×20 µm and smaller. Crystalline quality of superlattice is characterized using high resolution x-ray diffraction and the FWHM of zeroth order peak can reach below 20 arcsec. Occasionally, samples are measured under the TEM to verify the abrupt interfaces and the straight atomic layers, as shown in Figure 3(b).

Device fabrication and testing

For good quality materials, we process them into single element diodes and check the electrical and optical quality. First, we define the mesa isolation pattern by standard UV photolithography, using a mask featuring devices with sizes ranging from 400 to 100 µm. Most of the superlattice is etched in a BCl_3 based plasma using an Electron Cyclotron Resonance-Reactive Ion Etch (ECR-RIE) system. The etching is then completed using a citric acid based solution. After cleaning, top/bottom Ti/Pt/Au contacts are deposited using an electron beam metal evaporation system. Diodes were wire bonded, mounted with indium on leadless chip carrier, and loaded on the cold finger of a cryostat. Electrical and optical characterizations were performed using a set-up described elsewhere.[7]

For a recently designed superlattice of 13InAs/7GaSb with InSb interfaces, the 50% cutoff wavelength was measured to be ~12° µm at 77K. R_0A_{max} at 77K was reached 33 $\Omega \cdot cm^2$. Our optical measurements revealed an average detectivity and external quantum efficiency, reaching respectively $\sim 2\times 10^{11}$ Jones and 40-50%, as shown in Figure 4.

FPA processing and imaging

A similar material used for the up-to-date LWIR focal plane arrays has a 50% cutoff wavelength at 9.3 µm at 77K, longer than the previously demonstrated.[8,9] We first defined a 256×256 array of 25 µm×25 µm square mesas using the same etching technique described for single element devices. We cleaned carefully the surface of the array using warm photoresist stripper to remove photoresist residue. We then deposited the top\bottom Ti\Pt\Au contacts using a liftoff technique. The devices were then passivated using a combination of ammonium sulfide and SiO_2. Ammonium sulfide has been already shown to be an efficient electrical passivation layer for Type II superlattices[10]. In order to protect it against degradations due to other steps of FPA processing, 300 nm of SiO_2 was deposited on top using a Plasma Enhanced Chemical Vapor Deposition (PECVD) system. Windows were opened in the passivation using a HF based solution. The array was then hybridized to a 256×256 CMOS Litton ROIC with indium soldering bumps, deposited by a metal thermal evaporation system.[11] The gap between the array and the ROIC was sealed using epoxy to avoid foreign materials to penetrate in the gap and deteriorate the diodes. The GaSb substrate was then thinned down to a thickness of 20-30 µm using a lapping/polishing procedure. The FPA was loaded into a ceramic leadless chip carrier and wire bonded for testing.

The FPA testing was performed using a SE-IR infrared camera testing system between 80 K and 150 K, with a frame rate of 27.47 Hz, an integration time of 42 ms, and LWIR F/2 lens. Figure 5(a) shows the infrared image of a man with bad pixel replacement and two points uniformity correction, taken at 83 K. Most of the bad pixels correspond to the area seen in the center. They are not imaging because of a crack that appeared during the thinning down of the substrate. This defect may be due to the presence of a dust during the flip chip bonding or of an air bubble trapped during the edge sealing. When the array was thinned down to such a thickness of 20-30 µm, the substrate was not able to support the stress generated by the dust or the bubble anymore and cracked. The FPA was able to perform imaging of a hot soldering iron up to 150K Figure 5(b).

Conclusion

We have introduced a new concept of Type II "M" structure superlattice, and demonstrated high quality superlattice material growth and high performance single element detectors at liquid nitrogen temperature with cutoff wavelength around 12 µm. We have demonstrated the first of its kind FPA based on Type II InAs\GaSb with 50% cutoff around 9.3 µm, imaging from 80K up to 150K.

References

[1] G.A. Sai-Halasz, R. Tsu, and L. Esaki, Appl. Phys. Lett., 30, 651, 1971.

[2] D. L. Smith and C. Mailhiot, J. Appl. Phys. 62 (6), 2545 (1987).

[3] Yajun Wei, Aaron Gin, and Manijeh Razeghi, Gail J Brown, Appl. Phys. Lett., 81(19), 3675-3677 (2002).

[4] Manijeh Razeghi, Yajun Wei, Aaron Gin, Gail J. Brown, Daniel K. Johnstone, Proc. SPIE, 4650, 111-116, 2002.

[5] Yajun Wei, Manijeh Razeghi, Phys. Rev. B, 69, 085316-(1-7), 2004.

[6] Yajun Wei, Manijeh Razeghi, Gail J. Brown, Meimei Z. Tidrow, Proc. SPIE, 5359, 301-308, 2004.

[7] A. Gin, Y. Wei, A. Hood, A. Bajowala, V. Yazdanpanah, and M. Razeghi, Appl. Phys. Lett. 84, 2037 (2004).

[8] M. Razeghi, Y. Wei, J. Bae, A. Gin, A. Hood, J. Jiang, J. Nah, Proc. of SPIE, 5246, 501 (2003).

[9] Y. Wei, A. Hood, A. Gin, V. Yazdanpanah, M. Razeghi, M. Tidrow, Proc. SPIE, 5732, 309 (2005).

[10] A. Gin, Y. Wei, A. Hood, A. Bajowala, V. Yazdanpanah, and M. Razeghi, Appl. Phys. Lett. 84, 2037 (2004).

[11] M. Razeghi, Y. Wei, A. Hood, D. Hoffman, B. M. Nguyen, P. Y. Delaunay, E. Michel, R. McClintock, Proc. of SPIE, 6206 62060N-1 (2006).